International Journal of Electrical Engineering.
ISSN 0974-2158 Volume 9, Number 3 (2016), pp. 291-312

http://www.irphouse.com

Fuzzy Predictive Control of Three-Phase Four Switch Inverter-Fed Induction Motor Drives

Pala Prasad Reddy M.[1], Harinath Reddy K.[2], Swathi S.[3]

[1]Assistant professor, Dept. of EEE,
[2]Assistant professor, Dept. of EEE
[3]M.Tech (Electrical Power Engineering)

Abstract

The 4-switch three-segment (B4) inverter has the likelihood of lowering the inverter cost, and it grew to be very attractive in fault-tolerant manage to clear up the open/short-circuit faults of the six-change three-section (B6) inverter. Predictive control results in a fluctuation of the two dc-link capacitor voltages which factors the unbalance among the section currents. Predictive torque control (PTC) scheme is proposed for the B4 inverter-fed induction motor (IM) with the dc-link voltage offset suppression. For distinct prediction and manage of the torque and stator flux, the voltage vectors of the B4 inverter below the fluctuation of the 2 dc-link capacitor voltages are derived. With the aid of directly controlling the stator flux, the three-section currents are pressured to remain stability. The voltage offset of the 2 dc-link capacitors is modeled and managed within the predictive factor of view.

The simulation studies were carried out in the MATLAB/SIMULINK environment. In order to improve the performance of the IM drives, the PI controller is used to reduce the torque and stator flux ripples. For further improvement in the system performance a model free based approach i.e Fuzzy Logic Controller (FLC) is designed. The torque as well as stator flux ripples are considerably less in FLC approach compared to PI controller.

Keywords: Model Predictive Control (MPC), Induction Motor(IM), four switch inverter, cost function, current unbalance.

INTRODUCTION

Over time, the conventional three-segment voltage supply inverter with six switches (B6) has been discovered well known industrial functions in various varieties, similar to motor drives and energetic filters. However, in certain applications, a further cost reduction for inverter configuration is considered by users. To achieve this intention, the three-section inverter with simplest four switches was proposed via Van der Broeck and Van Wyk [1] for the reason of minimizing the add-ons' cost, and it is named 4-switch three-segment (B4) inverter in assessment with the B6 one, The illustration is detailed shown in Figure 1. Even though this type of fee reduction is on the cost of output efficiency, the B4 inverter can also be utilized in fault-tolerant manipulate to clear up the open/quick-circuit fault of the B6 inverter. The enhanced idea of said B4 inverter applied to fault-tolerant control is very strong and valuable in some critical occasions such as rail traction, and it has consequently attracted the interest of many researchers [2],[3].

We have several Disadvantages when compared with normal six switch inverters with four switch inverters. The voltage utilization factor is halved compared to the six-switch inverter.The balanced phase motor provides tap voltage in centre with fluctuating, and it destroys the balance among the motor phase currents [4]. The capacitor center tap voltage fluctuation increases as the load torque becomes higher or the frequency of a B4 inverter becomes lower, and the unbalanced motor current leads to an inverter failure and torque pulsation.

In order to mitigate the effects of the capacitor center tap voltage fluctuation, several papers were published [5],[6]. Microprocessors are increasing in very fast and powerful as the development is increasing the attention of various dedicated model predictive control (MPC) in power electronics [7].

The first ideas about this strategy applied to power converters started in the 1980s [8], [9].

The main concept is based on calculating the system's future behaviour to obtain optimal values for the actuating variables. With this intuitive concept, predictive control can be applied to a variety of systems, in which constraints and nonlinearities can be easily included, multivariable case can be considered, and the resulting controller is easy to implement.

In the PTC, the complete model and future behaviour of the inverter-fed drives are taken into account. A cost function relating to torque and flux errors reduction is defined to evaluate the effects of each voltage vector and the one minimizing the cost function is selected [10],[11].

In the outstanding performance of various B6 inverter-fed drives based on the PTC, PTC for B4 inverter-fed drives did not get many attentions to the researchers. Some simulation results of PTC for the B4 inverter-fed drives emulating the B6 case were carried out in [11]. However, the dc-link voltages fluctuation, which is the intrinsic feature of the B4 inverter, was not considered.

Additionally, and the offset suppression of the two capacitor voltages was not mentioned.

In proposed paper various special issues are providing and using the famous PTC control scheme for B4 inverter-fed IM drives are analyzed and discussed. Considering the fact that of the halved swap states akin to B6 one, the real-time implementation time rate for the percent scheme in B4 inverter is decreased in a sampling interval.

II. B4 INVERTER AND IM MODELING

A. Intrinsic Voltage Vector of a B4 Inverter

Fig.1 shows the B4 topology having a two leg inverter in which switches(T1 – T4) are considered ideal (i.e., no saturation voltage drop and no dead time) for our convenient analysis. S_b and S_c can be used as binary state variables to denote the switching states of leg b (T1,T2) and leg c (T3,T4) respectively. The dc-link is split in to two voltage sources, one load phase is connected to the middle of dc-link. The simultaneous closed states of two switches in each leg is usually avoidable inorder to prevent the short circuit of dc-link. Therefore, binaries 1 and 0 will indicate the closed states of upper switch and lower switch respectively. By assuming the three-phase voltages as balanced, the phase-to-neutral voltages V_{aN} ,V_{bN} ,V_{cN} are as follows:

$$V_{aN} = \frac{V_{dc1}}{3}(-S_b - S_c) + \frac{V_{dc2}}{3}(2 - S_b - S_c)$$

$$V_{bN} = \frac{V_{dc1}}{3}(2 - S_b - S_c) + \frac{V_{dc2}}{3}(2 - S_b - S_c - 1)$$

$$V_{cN} = \frac{V_{dc1}}{3}(2 - S_c - S_b) + \frac{V_{dc2}}{3}(2 - S_c - S_b - 1) \qquad (1)$$

Where V_{dc1} and V_{dc2} are the upper and the lower dc-link capacitor voltages, respectively.

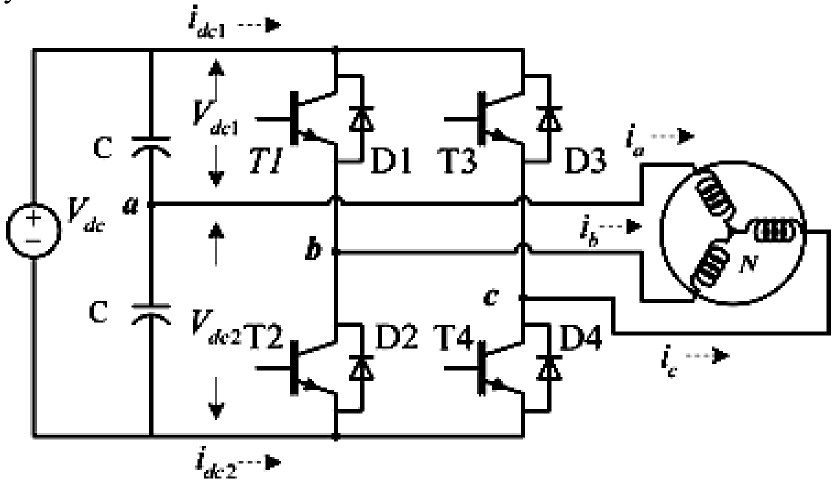

Fig.1: Circuit diagram of B4 inverter-fed Induction motor drive

Table I gives the phase-to- neutral voltages values by considering all the possible combinations of (S_b ,S_c).

The Clarke transform applied to the stator voltages yields as follows:

$$\begin{bmatrix} V_{\alpha s} \\ V_{\beta s} \end{bmatrix} = \frac{2}{3}\begin{bmatrix} 1 & -\frac{1}{2} & -\frac{1}{2} \\ 0 & \frac{\sqrt{3}}{2} & -\frac{\sqrt{3}}{2} \end{bmatrix}\begin{bmatrix} V_{aN} \\ V_{bN} \\ V_{cN} \end{bmatrix} \qquad (2)$$

where the $V_{\alpha s}$ and $V_{\beta s}$ are the α- and β-axis stator voltage, respectively. The voltage vectors are expressed by $\vec{v_s} = V_\alpha + jV_\beta$.

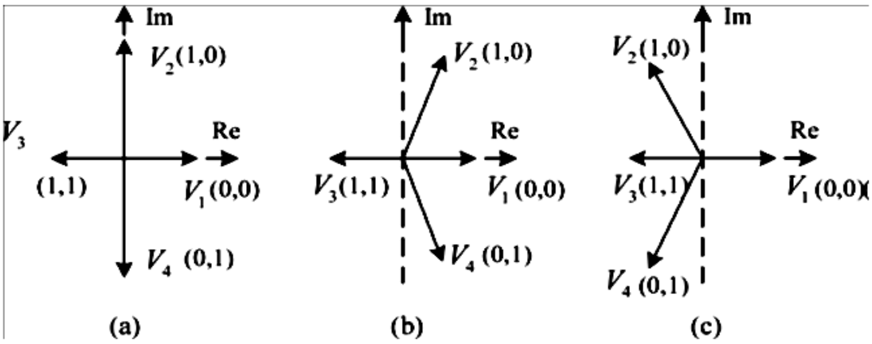

Fig.2. Basic voltage vectors of theB4 inverter(a) $V_{dc1} = V_{dc2}$ (b) $V_{dc1} < V_{dc2}$ and (c) $V_{dc1} > V_{dc2}$

It can be seen clearly that in Table II which gives the four active voltage vectors(V1-V4) in the $\alpha\beta$ plane, the B4 inverter can only produce four basic nonzero voltage vectors.

Table I. B4 Inverter Switching Functions and Output Voltages

States		Switch on		Output Voltage		
S_b	S_c			V_{aN}	V_{bN}	V_{cN}
0	0	T2	T4	$2V_{dc2}/3$	$-V_{dc2}/3$	$-V_{dc2}/3$
0	1	T2	T3	$(V_{dc2}-V_{dc1})/3$	$-(2V_{dc2}+V_{dc1})/3$	$(V_{dc2}+2V_{dc1})/3$
1	0	T1	T4	$(V_{dc2}-V_{dc1})/3$	$(V_{dc2}+2V_{dc1})/3$	$-(2V_{dc2}+V_{dc1})/3$
1	1	T1	T3	$-2V_{dc1}/3$	$V_{dc1}/3$	$V_{dc1}/3$

Fig.2(a) represents the four voltage vectors when the values of the upper and lower capacitance are big enough to keep the capacitor voltages a constant value of $V_{dc}/2$.

Fig.2(b) and (c) presents the vector positions in the conditions of $V_{dc1} < V_{dc2}$ and $V_{dc1} > V_{dc2}$ respectively.

Table II. Basic Voltage vectors of the B4 Inverter

Switching states (S_b. S_c)	Voltage Vectors ($\overrightarrow{v_s}$)	Vector Symbol
00	$2V_{dc2}/3$	V1
10	$(V_{dc2}-V_{dc1})/3-j\sqrt{3}((V_{dc2}+V_{dc1})/3$	V2
11	$(V_{dc2}-V_{dc1})/3+j\sqrt{3}((V_{dc2}+V_{dc1})/3$	V3
01	$-2V_{dc1}/3$	V4

B. Machine Equations

Stator variables, voltage $\overrightarrow{v_s}$, current $\overrightarrow{\iota_s}$, and flux $\overrightarrow{\varphi_s}$ are electrically related according to

$$\overrightarrow{v_s} = R_s\overrightarrow{\iota_s} + \frac{d\overrightarrow{\varphi_s}}{dt} \tag{3}$$

where Rs is the stator resistance.

Rotor equation in a stator reference frame represents the relation between rotor current $\overrightarrow{\iota_r}$ and rotor flux $\overrightarrow{\varphi_r}$ as follow

$$0 = R_r\overrightarrow{\iota_r} + \frac{d\overrightarrow{\varphi_r}}{dt} - j\omega\overrightarrow{\varphi_r} \tag{4}$$

where Rr is the rotor resistance and ω is the rotor speed.

Flux linkage equations relate stator and rotor currents are given in (5) and (6), where L_m, L_s and L_r are the mutual, stator, and rotor inductances, respectively

$$\overrightarrow{\varphi_s} = L_s\overrightarrow{\iota_s} + L_m\overrightarrow{\iota_r} \tag{5}$$

$$\overrightarrow{\varphi_r} = L_m\overrightarrow{\iota_s} + L_r\overrightarrow{\iota_r} \quad (6)$$

Electromagnetic torque *Te* can be expressed in terms of stator current and stator flux

$$T_s = \frac{3}{2}p\overrightarrow{\varphi_s} \times \overrightarrow{\iota_s} \quad (7)$$

where p is the number of pole pairs.

The ratio of change in the mechanical rotor speed ω by the Torque

$$J\frac{d\omega}{dt} = T_e - T_L \quad (8)$$

where the coefficient J denotes the moment of inertia of the mechanical shaft, and T_L is the load torque to the machine.

III. ALGORITHM FOR THE PTC SCHEME

Proposed Algorithm named three-step algorithm provides a facility to carry out in any standard “PTC SCHEME”: in this cost estimation optimization is linked with flux and torque [10]. In the provided structure of B4 inverter-fed “IM drive-based PTC scheme” is detailed shown in Fig. 3 in which the inner loop is a stator flux and electromagnetic torque controller based on PTC, while the outer speed loop is a traditional PI controller.

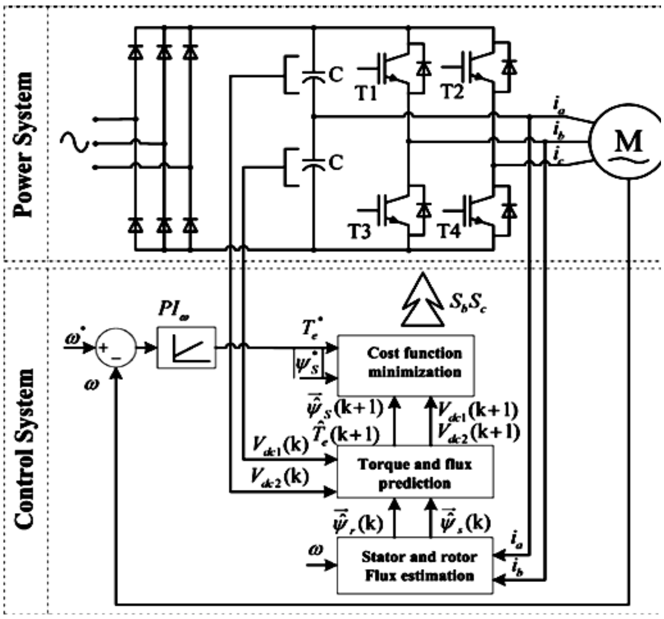

Fig.3. Structure of the B4 inverter-fed IM drive based on the PTC scheme.

A. Flux Estimation

The dc-link voltage ripple existence in the B6 inverter means a proportional alteration of all three output phase voltages and accordingly an amplitude error of the average voltage vector used. Whereas in a B4 inverter, the voltage ripple leads to different modification of the voltages on the three phase (see Table I) and to both amplitude and angular errors of the switching voltage vectors. Moreover, a significant fluctuation of the dc-link voltages is inevitable due to one-phase current flows through the split dc-link voltage sources. Hence, the voltage-model-based flux estimator using the command voltages becomes less accurate in the B4 case whereas in the B6case, it can approximately estimate the stator flux [10].

Current-model-based flux estimator using instant currents and speed signals are adopted in the proposed scheme and at the present sampling step k the estimations of the stator flux $\overrightarrow{\varphi_s}$ and the rotor flux $\overrightarrow{\varphi_r}$ are required. The rotor flux can be calculated using equivalent equation of an induction machine.

$$\overrightarrow{\varphi_r} + \tau_r \frac{d\overrightarrow{\varphi_r}}{dt} = -j\tau_r(\omega_k - \omega)\overrightarrow{\varphi_r} + L_m\overrightarrow{\iota_s} \tag{9}$$

where $\tau_r = \frac{L_r}{R_r}$, $\boldsymbol{\omega}_k$ the angular speed of a rotating coordinate frame, and ω corresponds to the rotor speed.

Writing (9) in terms of a rotating reference frame aligned with the stator winding ($\boldsymbol{\omega}_k = 0$) is given as follows:

$$\overrightarrow{\varphi_r} + \tau_r \frac{d\overrightarrow{\varphi_r}}{dt} = L_m\overrightarrow{\iota_s} + j\omega T_r\overrightarrow{\varphi_r} \tag{10}$$

For the stator flux estimation, the rotor linkage (6) is used to write the rotor current in terms of the measured stator currents and the estimated rotor flux.

Then, by replacing $\overrightarrow{\iota_r}$ of (6) in the stator flux (5), the stator flux estimation is obtained

$$\overrightarrow{\varphi_s} = L_m\left(\frac{\overrightarrow{\varphi_r} - L_m\overrightarrow{\iota_s}}{L_r}\right) + L_r\overrightarrow{\iota_r} \tag{11}$$

Using Euler-based discretization in (10) and (11), the discrete equations of the rotor and stator flux estimation are as follows:

$$\overrightarrow{\widehat{\varphi_r}}(k) = \frac{T_r}{T_s(1 - j\omega T_r)}\overrightarrow{\varphi_r}(k-1) + \frac{L_m}{1 - j\omega T_r}\overrightarrow{\iota_s}(k)(12) \tag{12}$$

$$\overrightarrow{\widehat{\varphi_s}}(k) = k_r\overrightarrow{\widehat{\varphi_r}}(k) + \sigma L_s\overrightarrow{\iota_s}(k)\ (13) \tag{13}$$

Where T_s corresponds to the sampling time, $K_r = L_m / L_r$ is the rotor coupling factor and $\sigma = 1 - (\frac{L_m^2}{L_m L_s})$ is the total leakage factor.

The rotor flux estimation is obtained without using the command voltages in (12).

Thus, the accurate flux estimation for the B4 inverter-fed IM is achieved.

B. Stator Flux and Electromagnetic Torque Prediction

Stator flux and electromagnetic torque are the control variables, so that their behaviours must be predicted at sampling step $k + 1$.

The stator flux prediction $\overrightarrow{\hat{\varphi}_s}(k+1)$ is obtained by the stator voltage equation.

Using the Euler formula to discretize (3) and shifting the result to a single time step, the stator flux prediction is obtained

$$\overrightarrow{\hat{\varphi}_s}(k+1) = \overrightarrow{\hat{\varphi}_s}(k) + T_s \overrightarrow{v_s}(k) - R_s T_s \overrightarrow{\iota_s}(k) \tag{14}$$

where Ts is the sampling time used in the PTC algorithm.

The electromagnetic torque prediction can be calculated as

$$\hat{T}_e(k+1) = \frac{3}{2} p \cdot Im\{\overrightarrow{\hat{\varphi}_s}(k+1) \cdot \overrightarrow{\iota_s}(k+1)\} \tag{15}$$

The prediction expression of the stator current $\overrightarrow{\iota_s}(k+1)$ is obtained using the equivalent equation of the stator dynamics of an induction machine

$$\overrightarrow{v_s} = R_s \overrightarrow{\iota_s} + L_\sigma \frac{d\overrightarrow{\varphi_s}}{dt} - k_r (\frac{1}{T_r} - j\omega) \overrightarrow{\varphi_r} \tag{16}$$

where $R_\sigma = R_s + K_r^2 R_r$ corresponds to the equivalent resistance and $L_\sigma = \sigma L_s$ is the leakage inductance of the machine.

The last term in (16) represents the cross coupling between the rotor and the stator winding through the induced voltage. Thus, replacing the derivatives with the Euler formula in (16), the prediction equation of the stator current $\overrightarrow{\iota_s}$ at the instant $k + 1$ is obtained .

$$\vec{\iota_s}(k+1) = \left(1 + + \frac{T_s}{\tau_\sigma}\right)\vec{\iota_s}(k) + \frac{T_s}{\tau_\sigma + T_s}\{\frac{1}{R_\sigma}\left(\left(\frac{k_r}{\tau_r} - j\omega k_r\right)\overrightarrow{\varphi_r}(k) + \vec{v_s}(k)\right)\} \quad (17)$$

After obtainin the predictions of the stator flux (14) and the stator current (17), the prediction of the electromagnetic torque can be calculated in (15).

C. Cost Function Optimization

The next step in predictive control is the optimization of an appropriate control law that is defined as a cost function. The structure form of the cost function is given as follows:

$$g_i = \frac{\left|T_e^* - \widehat{T}_e(k+1)_i\right|}{T_{e_{nom}}} + \lambda_0 \frac{\left|\|\overrightarrow{\varphi_s^*}\| - \|\widehat{\overrightarrow{\varphi_s}}(k+1)_i\|\right|}{\|\overrightarrow{\varphi_s}\|_{nom}}$$

$$i \in \{1,2,3,4\} \quad (18)$$

where *i* denotes the index of the stator voltage vector used to calculate the predictions $\widehat{T}_e(k+1)$ and $\widehat{\varphi_s}(k+1)$, respectively.

The rated torque $T_{e_{nom}}$ and the rated stator flux magnitude $\|\overrightarrow{\varphi_s}\|_{nom}$ are used to normalize the cost function terms. The torque reference is externally generated by a PI speed controller. The factor λ_0 denotes a weight factor. Finally, the optimization step is carried out, and the inverter voltage vector that minimizes the cost function is selected as the optimal switching state for the next sampling period $k + 1$, thus the optimal torque and flux control is achieved.

D. Time-Delay Compensation

It is well known that there is one-step delay in digital implementation. In other word, the voltage vector selected at the instant time k will not be applied until the instant time $k + 1$ [10]. To eliminate this delay, the value at the instant time $k + 2$ should be used in (18) rather than the instant time $k + 1$. Therefore, the cost function (18) is redefined as

$$g_i = \frac{\left|T_e^* - \widehat{T}_e(k+2)_i\right|}{T_{e_{nom}}} + \lambda_0 \frac{\left|\|\overrightarrow{\varphi_s^*}\| - \|\widehat{\overrightarrow{\varphi_s}}(k+2)_i\|\right|}{\|\overrightarrow{\varphi_s}\|_{nom}}$$

$$i \in \{1,2,3,4\} \quad (19)$$

E. DC-Link Voltage Offset Suppression

The inappropriate initial phase angle of phase “a” current or the imbalance current flowing in the two capacitors will cause voltage deviation [5]. Therefore, suppressing the offset of the two capacitor voltages is necessary.

$$g_i = \frac{|T_e^* - \widehat{T_e}(k+2)_i|}{T_{e_{nom}}} + \lambda_0 \frac{\left|\|\overrightarrow{\varphi_s^*}\| - \|\overrightarrow{\widehat{\varphi_s}}(k+2)_i\|\right|}{\|\overrightarrow{\varphi_s}\|_{nom}} + \lambda_{dc} \frac{|\widehat{V_{dc1}}(k+1)_i - \widehat{V_{dc2}}(k+2)_i|}{V_{dc}}$$

$i \in \{1,2,3,4\}$ (20)

Where $V_{dc}$is dc-link voltage, which can be obtained by $V_{dc}=V_{dc1}+V_{dc2}$, λ_{dc} is the weight factor of the dc-link capacitor voltage offset suppression. By an exhaustive search for all feasible voltage vectors, the minimization of (24) is done. The proposed control scheme can be implemented in the following sequence as shown in Fig.4.

The superscript k, $k+1$, and $k+2$ denote the variables' value at sampling time k, $k+1$, and $k+2$, respectively.

$\overrightarrow{v_{opt}^{k}}$ and $\overrightarrow{v_{opt}^{k+1}}$are the optimal voltage vectors found in the previous loop iteration and the current loop iteration, respectively.

As it is shown earlier, a high degree of flexibility is obtained with the proposed control scheme due to the online optimization algorithm, where the system nonlinearities and restrictions (i.e., capacitor voltage offset suppression) can be included in the cost function.

IV. ANALYSIS OF WEIGHTING FACTORS

Weighting factor are the only parameters that are supposed to adjust in the proposed scheme which is clear from (24). Effect of the weighting factors can be analysed by performing the extensive simulation in MATLAB/Simulation. Table III shows the ratings and parameters of the B4 inverter and IM.

A. Stator Flux Weighting Factor λ_0

Weighting factor(λ_0) increases or decreases the relative importance of the torque versus flux control. λ_0= 1 if the same importance is assigned to both control objectives. A higher weighting factor λ_0 is expected (e.g., λ_0 = 3) to obtain the balanced currents versus the unbalanced structure of B4 inverter. Fig.5 shows the simulation results During a speed-reversal from 500 to –500 r/min at 50% rated load torque for the case of λ_0=3 where the stator flux reference is the nominal one at 0.6Wb. A comparable study for the same system is made with smaller weighting factor, λ_0 = 1 are presented in Fig.6. Here, it can be appreciated that the flux exhibits a higher ripple during steady state when compared to the previous case. During the transient, the balanced three-phase currents collapse due to the failure in stator flux control.
So, considering the good performance, in the remaining tests, the tuning factors λ_0 will be kept at the value of λ_0 = 3.

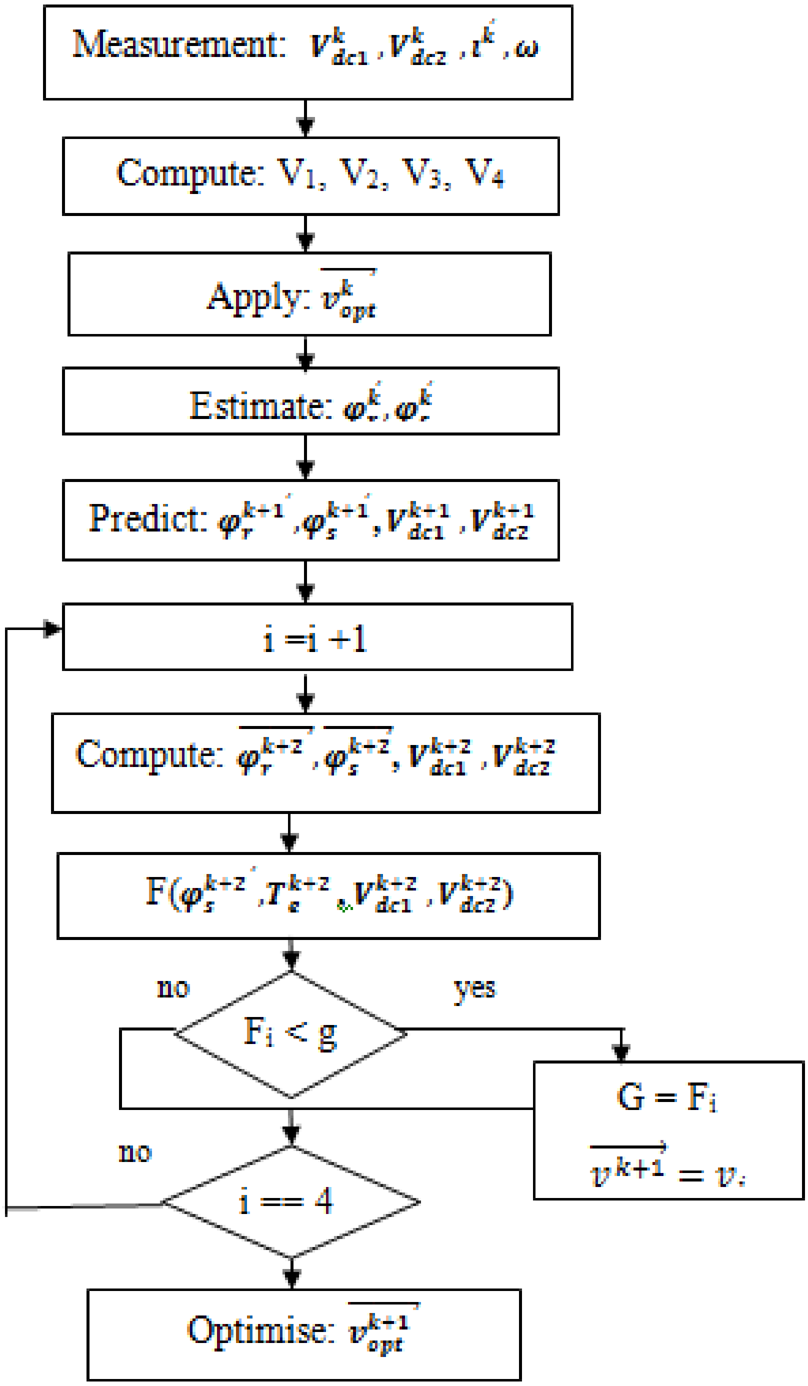

Fig.4. Implementation flowchart of the proposed scheme

Table III. Parameters of B4 inverter and IM

PARAMETERS	RATINGS
DC-link voltage	540 V
DC-link upper capacitor ($C1$)	2040 μF
DC-link upper capacitor ($C2$)	2040 μF
Dead time	4 μs
Induction Motor	
Rated power	2.2 kW
Rated voltage	380 V
Rated speed	1430 r/min
Rated current	4.9 A
Rated frequency	50 Hz
Number of poles	4
Stator resistance (Rs)	2.804 Ω
Stator leakage inductance (Ls)	10.33 mH
Rotor resistance (Rr)	2.178 Ω
Rotor leakage inductance (Lr)	10.33 mH
Magnetizing inductance (Lm)	319.7 mH
Nominal flux-linkage	0.6 Wb
Rated torque	14 N·m

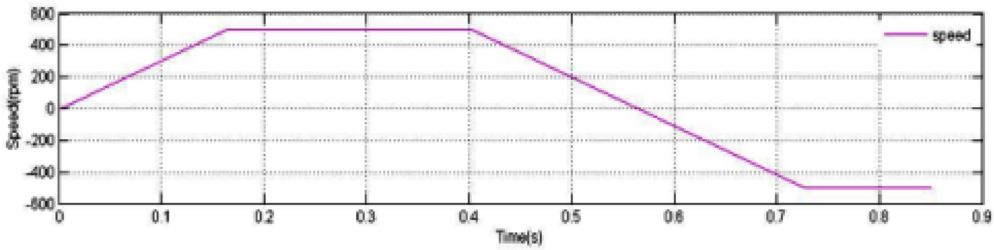

(a)

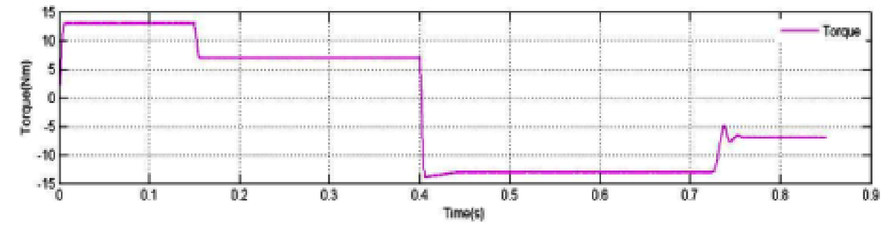

(b)

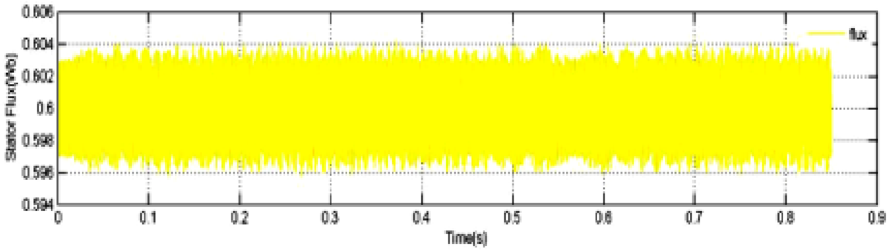

(c)

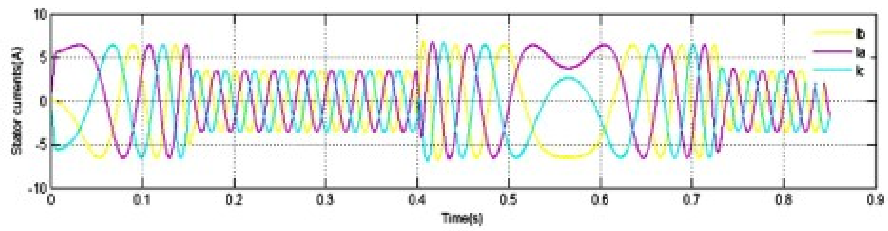

(d)

Fig.5. Simulated waveforms using the PTC with PI controller scheme for a B4 Inverter for λ_0=3 (a)Speed (b)Torque (c)Stator Flux (d)Stator Currents

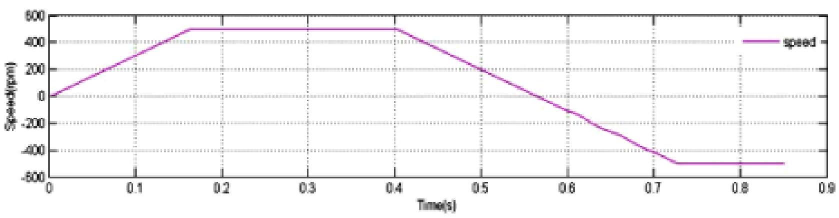

(a)

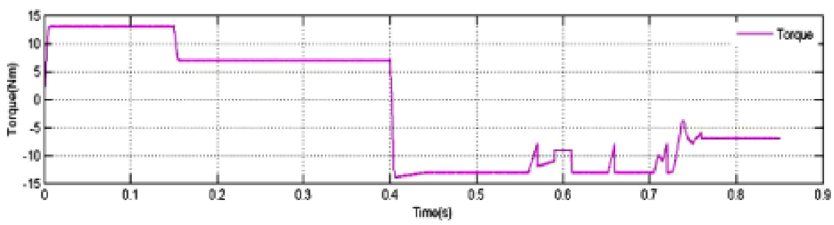

(b)

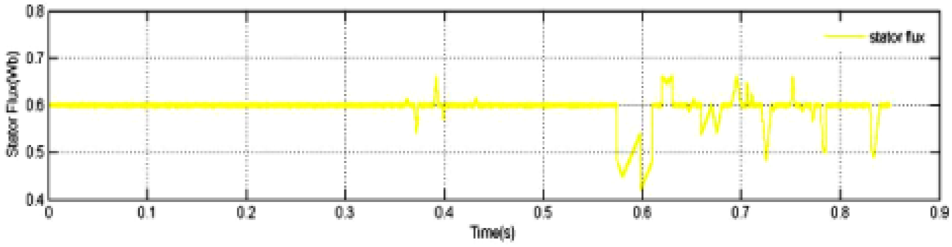

(c)

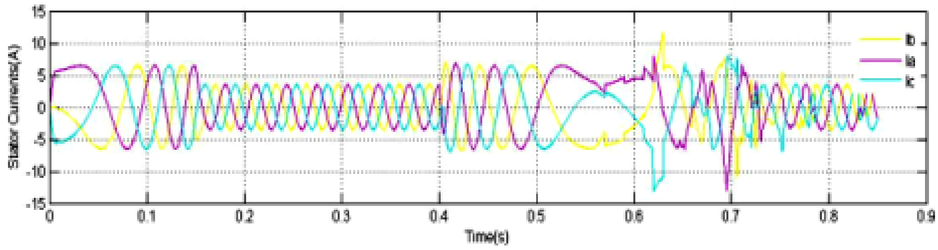

(d)

Fig.6. Simulated waveforms using the PTC scheme with PI controller for a B4 inverter for λ_0=1 (a)Speed (b)Torque (c)Stator Flux (d)Stator Currents

B. Capacitor Voltages Offset Suppression Weighting Factor λ_{dc}

The weighting factor λ_{dc} increases or decreases the relative importance of the dc-link capacitor voltage offset suppression versus the control performance. With a higher value of the weighting factor λ_{dc}, the two capacitor voltages converge faster, but when a very high value of this weighting factor is applied, the control performance is affected.

The simulation results at the speed of 500 r/min with a torque of 10Nm are shown in Figs. (7) and (8) in case of λ_{dc} =1000 and λ_{dc} = 2000, respectively.

In Fig.7, after the voltage offset suppression term is added at t=3s, the two capacitor voltages converge to 270V at t=7s, and as it is shown that a slight increment in the torque ripple occurs when the capacitor voltage offset term is added. This is acceptable with negligible effect on the flux and speed waveforms. For a comparative study, the results in the cases of λ_{dc} =2000 are shown in Fig.8. It can be noticed that the converging time of the two capacitor voltages is approximately 1s, but a significant stator flux and torque ripples are exhibited in the steady state. In consideration of the good performance obtained, in the remaining tests, the tuning factors λ_{dc} will be kept at the value of λ_{dc} = 1000.

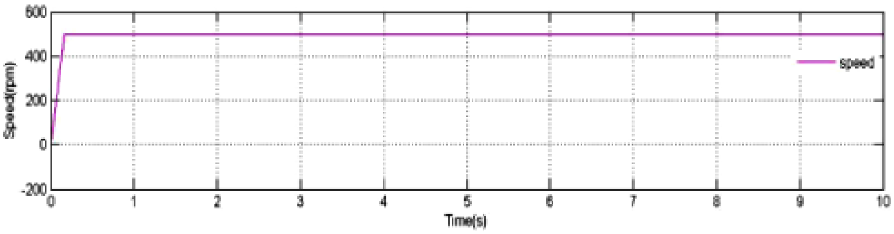

(a)

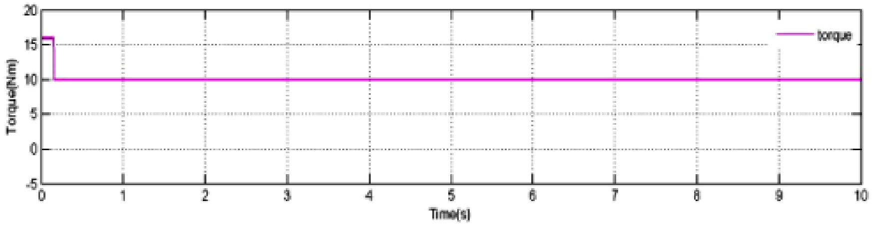

(b)

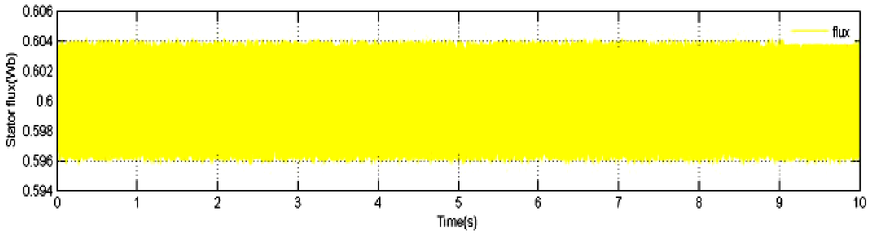

(c)

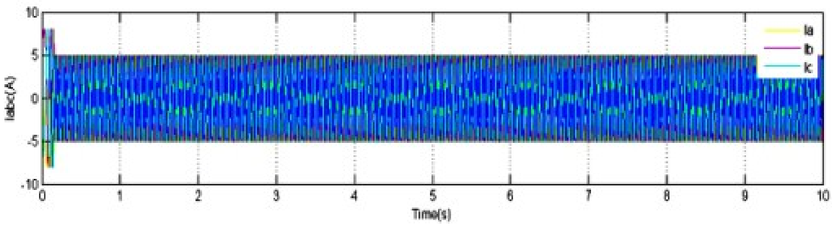

(d)

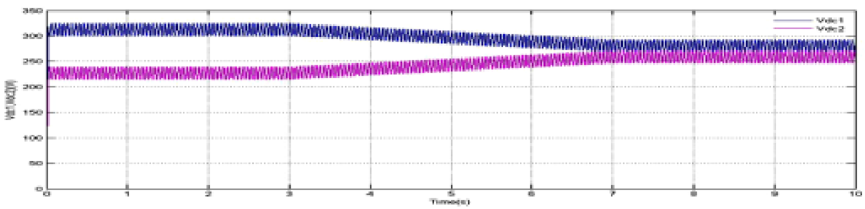

(e)

Fig.7. Simulated waveforms using the PTC scheme with PI controller withλ_{dc}=1000
(a)Speed (b)Torque (c)Stator Flux (d)Stator Currents (e)Capacitor Voltages

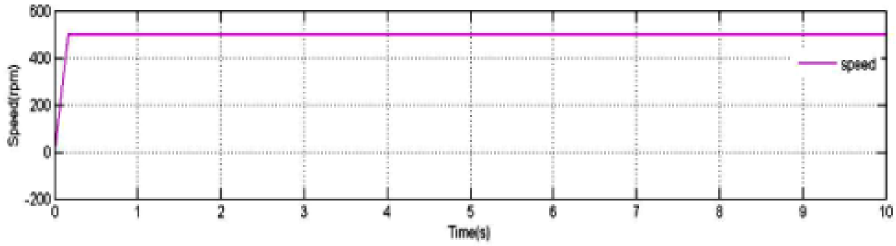

(a)

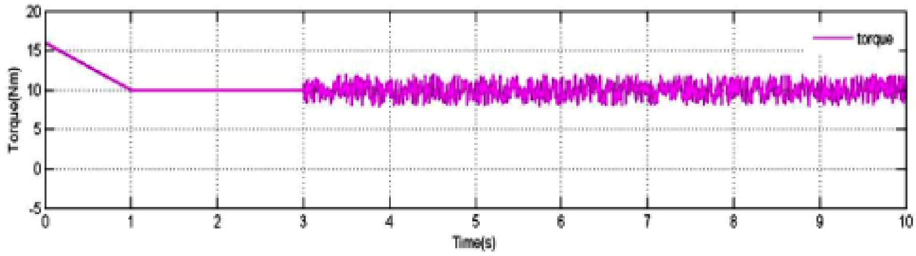

(b)

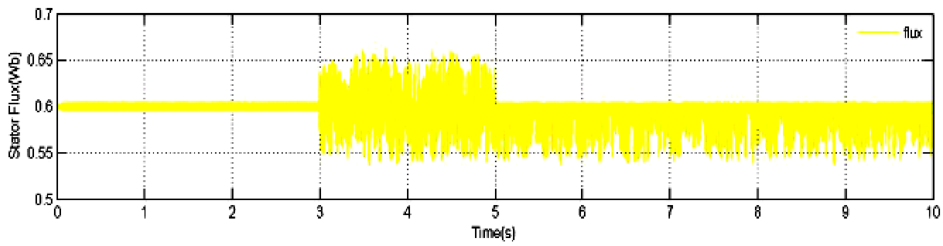

(c)

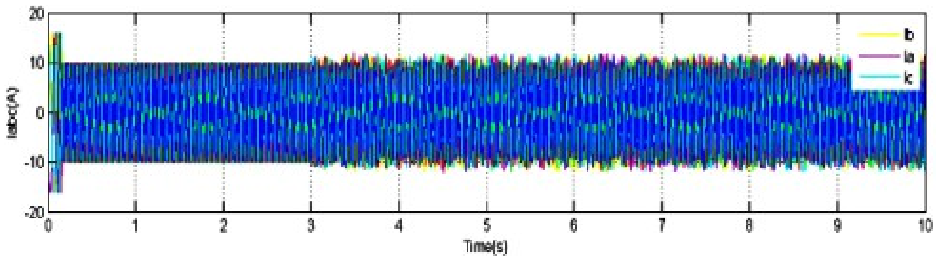

(d)

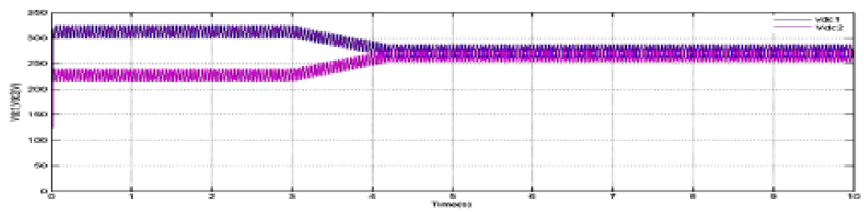

(e)

Fig.8. Simulated waveforms using the PTC scheme with PI controller with λ_{dc}=2000 (a)Speed (b)Torque (c)Stator Flux (d)Stator Currents (e)Capacitor Voltages

VI. FUZZY CONTROLLING SPEED LOOP

Fuzzy logic concept is a most efficient artificial intelligence method which has high application in electric motor drives. Depending on an operator's experience an algorithm of non-mathematical decision making is called Fuzzy logic control. It is an intelligent controller and its design does not depend on accurate mathematical model of the system. Rather than exact or fixed reasoning, the fuzzy logic deals with approximate many valued logic rules as shown in table IV.
A method to achieve fastest dynamic performance by modifying the two leg inverter fed PTC of induction motor based on Fuzzy Logic Controller is used in place of PI controller. With the usage of the Fuzzy logic concept, the reliability, efficiency and performance of ac drive increases. Initial torque peak and torque ripple are minimized in the four switch three phase inverter based DTC using Fuzzy Logic.

Table IV. Fuzzy Logic Rules

	NB	NM	NS	Z	PS	PM	PB
NB	PB	PB	PM	PM	PS	PS	Z
NM	PB	PM	PM	PS	PS	Z	NS
NS	PM	PM	PS	PS	Z	NS	NS
Z	PM	PS	PS	Z	NS	NS	NM
PS	PS	PS	Z	NS	NS	NM	NM
PM	PS	Z	NS	NS	NM	NM	NB
PB	Z	NS	NS	NM	NM	NB	NB

The simulation results are shown for the weighting factors $\lambda_0 = 1$, $\lambda_0 = 3$, $\lambda_{dc} = 1000$ and $\lambda_{dc} = 2000$ in fig. (9),(10),(11) and (12) respectively.

By analyzing the waveforms it is clear that the torque and current ripple is reduced.

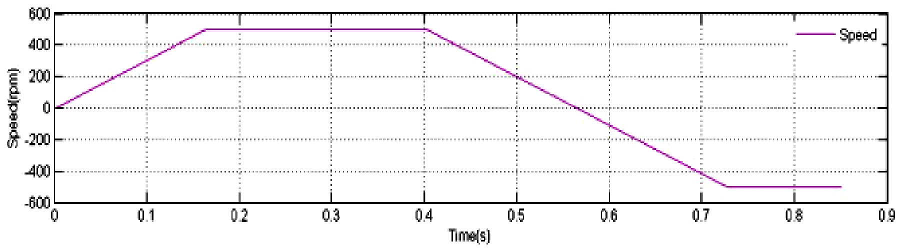

(a)

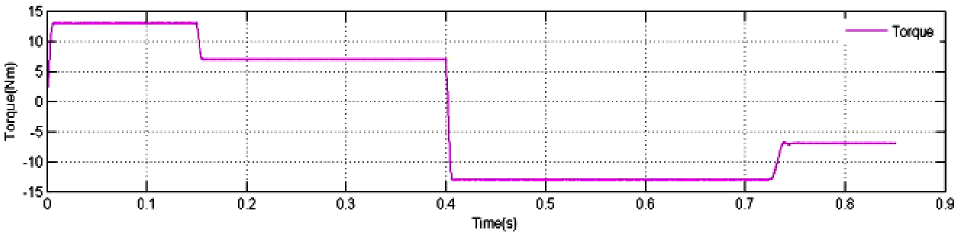

(b)

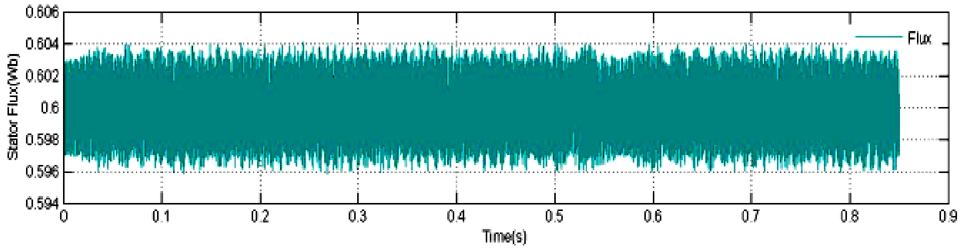

(c)

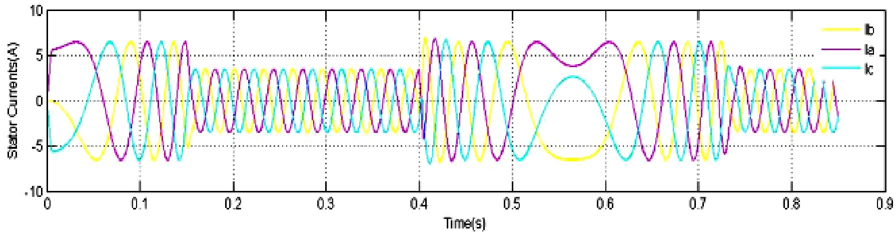

(d)

Fig.9. Simulated waveforms using the PTC scheme with fuzzy controller for a B4 Inverter for λ_0=3 (a)Speed (b)Torque (c)Stator Flux (d)Stator Currents

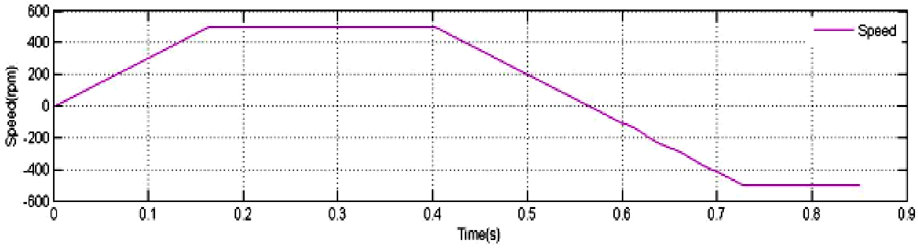

(a)

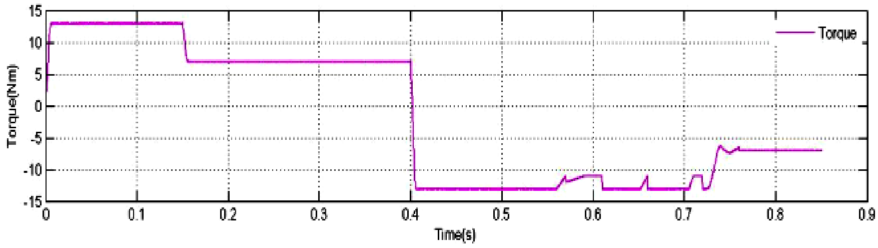

(b)

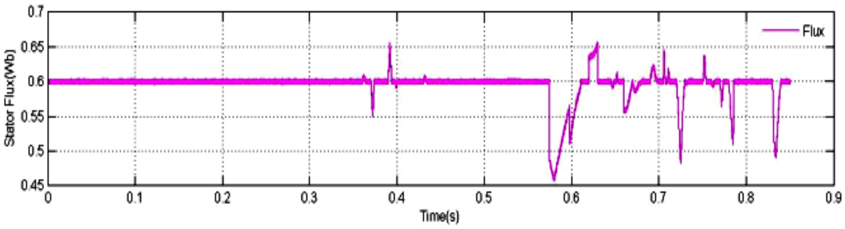

(c)

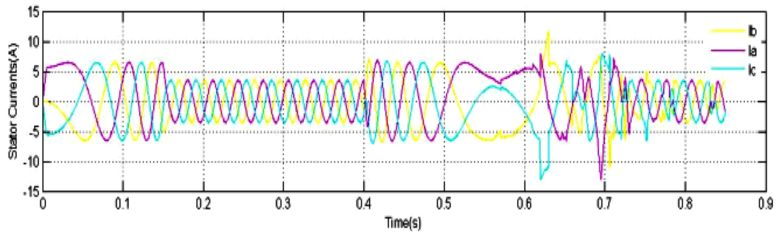

(d)

Fig.10. Simulated waveforms using the PTC scheme with fuzzy controller for a B4 inverter for λ_0=1 (a)Speed (b)Torque (c)Stator Flux (d)Stator Currents

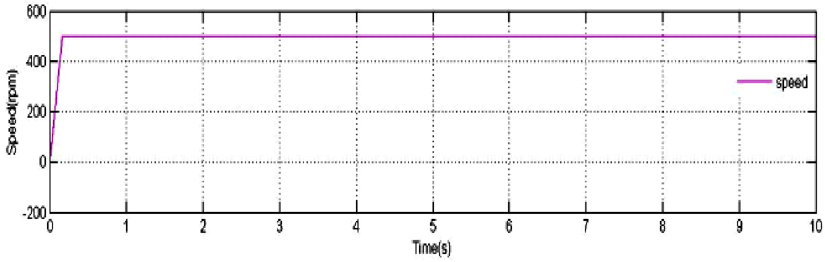

(a)

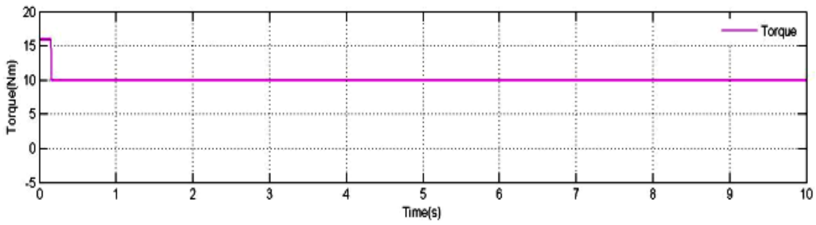

(b)

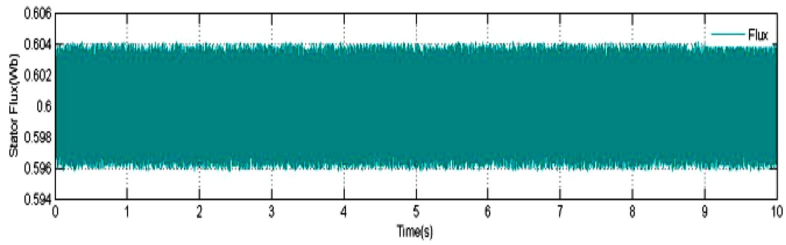

(c)

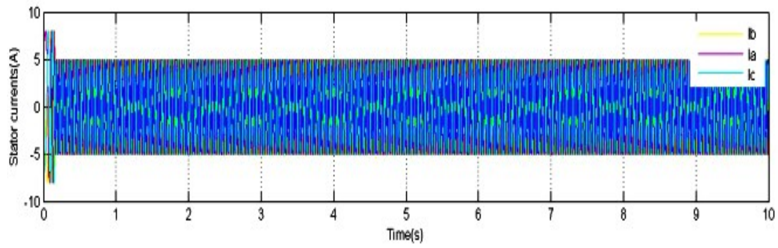

(d)

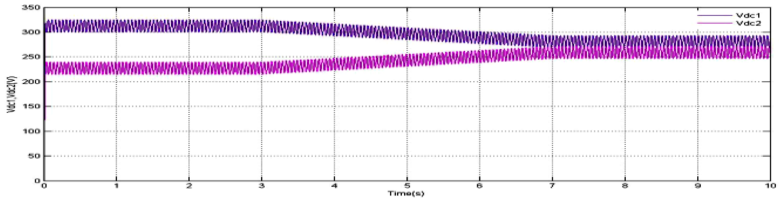

(e)

Fig.11. Simulated waveforms using the PTC scheme with fuzzy controller withλ_{dc}=1000 (a)Speed (b)Torque (c)Stator Flux (d)Stator Currents (e)Capacitor Voltages

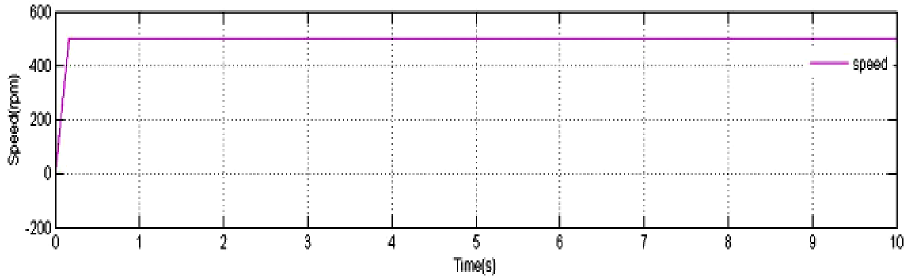

(a)

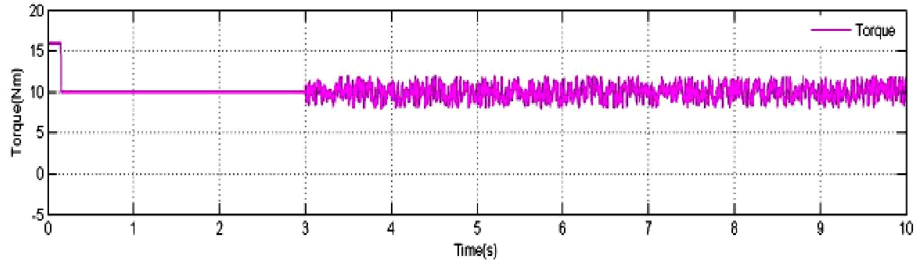

(b)

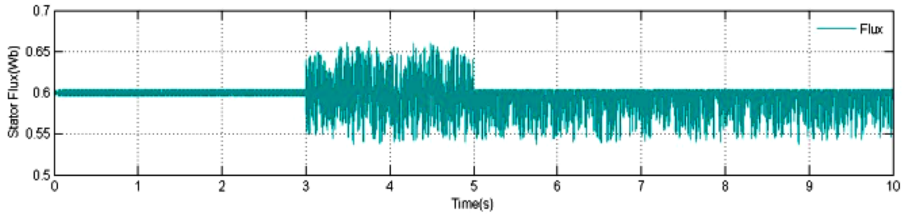

(c)

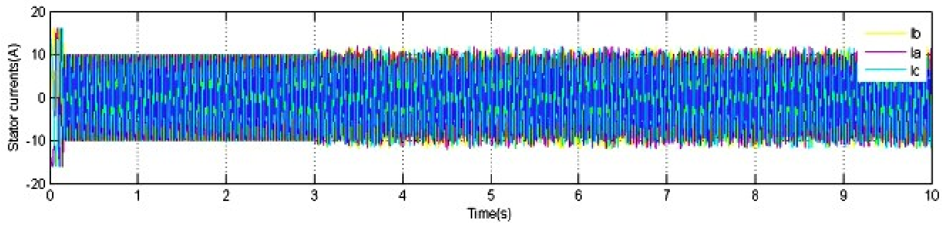

(d)

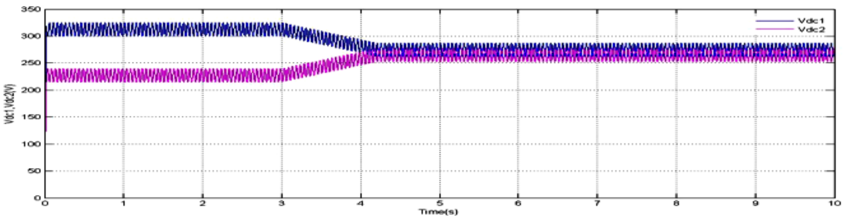

(e)

Fig.12. Simulated waveforms using the PTC scheme with fuzzy controller with λ_{dc}=2000 (a)Speed (b)Torque (c)Stator Flux (d)Stator Currents (e)Capacitor Voltages

VII. CONCLUSION

The B4 inverter fed IM drives is analysed and discussed. For the special prediction and manage of the torque and stator flux, the voltage vectors of the b4 inverter are derived beneath the fluctuations of the 2-link capacitor voltages. The investigation is carried out on the design and performance evaluation of the PTC scheme for the B4 inverter fed IM drive and achieved the balanced three-phase currents along with the suppression of capacitor voltage offset. Considering the cost reduction and its advantages, the proposed B4 inverter fed IM drive has been found acceptable for the high performance industrial variable-speed-drive applications. It has been observed that the torque and the stator flux ripples are reduced by using fuzzy controller in speed loop. Certainly, the additional work is still remained to develop more efficient PTC scheme when the question of parameter deviation is arised.

REFERENCES

[1]. H. Vander Breck and J. VanWayk, “A Detailed comparative investigation of a 3 phase induction system in drive with a enhanced component minimized voltage-fed inverter under different control options,” *IEEE Trans. Ind. App*, vol. IAA-220, no. 42, pp. 4309–2320, March/1984.

[2]. B. B. Welchkko, T. B. Lippo, P. M. Jaahns, and T. E. Scchulz, “tolerant fault three-phase AC motor:” *IEEE Trans Power Electron*, vol 2419, no. 44, ppp. 21108– 21116, Apr. 2004.

[3]. T. T. D. Ribeeiro, B. B. Jcoobina, T. T. C. da ESelva, and R. S. N. Lema, “Fault and tolerant voltage with fed PWM process and inverter drive system with AC,” *IEE Trans Ind.* vol. 351, 22, ppp. 44239–4346, Aug. 2004.

[4]. F.K. Balaabjerg, Y.D. P. Naeacsu, and F. K. Piedersen, “Optimized DC Link SVM voltage ripple for four-switch three-phase voltage-source inverters,” *IEEE Tranaction.*, vol. 114, no. 424, pp. 2743–4752, August. 1999.

[5]. R. T. Waango, J.R. Zoohao, and P.R. Lysiu, “A comprehensive fourswitch investigation of fourswitch wotj phase voltage in double Fourier integral,” *IEEE. Power Electron in IEEE.*, vol. 426, no. 210, pp. 422774–24787, November. 2011.

[6]. B. EP.l Baadsi, T.B. Biuouzidi, and O,T,Mousmaudi, "motor DTCscheme for a four-switch inverter-fed induction inverter operation emulating the six-switch," *IEE. Power Electron.*, vol. 328, no. 127, pp. 34528–33538, August. 2013.

[7]. P. A. Lae, "The three decades of Model predictive control: development," vol. 29, no. 233, pp. 4425–4214, April. 2011.

[8]. P.J. Haltz and P.R. Satradtfaldt, "Stator current vector A predictive controller for the of ac a switched voltage source machines fed from," in. *IEE IPEC*, 1993, vol. 22, pp. 2665–4675.

[9]. P.T.R. Konnel and T.D. Sesch¨oser, "for converters predictive control strategy," in *Proc. Control Power Electron. Elect. Drives*, 1988, pp. 3415–4422.

[10]. O.J. Rodaiguz, T.R. M. Konnel, Y.. O. Esinoza, M,B. Taincado, R. A. Sailva, and C. R.A. Ropjas, "performance High control strategies assessment," *IEE. Ind. Electron.*, vol. 359, no. 22, pp. 912–620, Jan. 2012.

[11]. P.P..Haabibullah and R. R. S. Loo, "control of afour Predictive torque and flux switch inverter-fed IM drive," in *Proc. Energy Electron.Conf.*, 2014, pp. 6229–6434.

AUTHOR PROFILE

[1]**M.Pala Prasad Reddy** completed B.Tech from JNTU Ananthapur in the year 2007. He also completed his Masters degree from NIT Calicut kerala in the year 2009. He is currently working as Asst. Professor at Annamacharya institute of technology and sciences, rajampet, kadapa dist, A.P., India. Optimization techniques, robust control schemes are his research areas of interest.

[2]**K.Harinath Reddy** completed B.tech from G.Pulla Reddy Engineering College, Kurnool in the year 2006. He also completed his Masters Degree from AITS, Rajampet in the year 2009. He is currently working as Asst. Professor at Annamacharya institute of technology and sciences, Rajampet, Kadapa dist, A.P., India.

[3]**S.Swathi** completed B.Tech from KSRM College of Engineering, kadapa in the year 2014. Currently Pursuing her Post Graduation in Electrical Power Engineering in AITS, Rajampet, Kadapa(dist.).